CRYSTAL GROWTH & DESIGN
2005
VOL. 5, NO. 4
1499−1507

Roles of Additives and Precipitants in Crystallization of Calcium- and Integrin-Binding Protein

Bryan W. Berger,[†] Chad J. Blamey,[‡,§] Ulhas P. Naik,[§] Brian J. Bahnson,[‡] and Abraham M. Lenhoff*[,†]

Center for Molecular and Engineering Thermodynamics, Department of Chemical Engineering, Department of Chemistry and Biochemistry, Department of Biological Sciences, University of Delaware, Newark, Delaware 19716

Received January 12, 2005; Revised Manuscript Received April 15, 2005

ABSTRACT: The interactions leading to crystallization of calcium- and integrin-binding protein (CIB), a novel Ca^{2+} binding protein, were characterized in terms of osmotic second virial coefficients, B_{22}, measured by self-interaction chromatography. In particular, the role of additives such as alkanediols or DMSO in improving crystal growth in the presence of sodium malonate, sodium formate, and sodium acetate was investigated. Short-chain alkane-1,*n*-diols were found to be effective in a range of 10−20% (v/v) in preventing CIB precipitation at the high sodium formate concentrations necessary for crystallization, whereas for alkane-1,2-diols longer chains were necessary, although at concentrations less than 5% (v/v). In both cases, significant improvement in protein crystal growth and suppression of precipitation were observed. Isothermal titration calorimetry measurements indicate that the differences in alkanediol specificity are a result of interactions with hydrophobic regions on the protein surface, which in turn depend on chain length and structure. Overall, our investigation of the protein−protein interactions provides valuable insight into the modulating roles that additives play, which is essential to developing rational approaches to protein crystallization. Our work also demonstrates the applicability of self-interaction chromatography to studying crystallization of novel proteins, particularly those that may otherwise be difficult to crystallize due to poor solubility.

Introduction

With the advent of structural genomics, the process of expressing and purifying proteins and determining their structures has seen rapid development in the past decade.[1] Figures taken from groups such as the Human Proteome Structural Genomics pilot program show that although more than half of the selected target sequences can be expressed and purified, fewer than 10% of these lead to successful structure determination. Of the purified proteins suitable for study, preliminary screening of crystallization conditions often leads to some crystal formation, but usually this information is inadequate to solve the structure to high resolution.[2] In particular, so-called "difficult proteins" emerge after purification as a large group. Generally, these proteins can be expressed and purified, although typically at lower levels than for most soluble proteins; additionally, many show poor solubility at the high concentrations necessary for crystallization.[3] Often this requires the presence of detergents such as *n*-octyl-*β*-D-glucoside or other amphiphilic additives such as 2-methyl-2,4-pentanediol (MPD) to reduce precipitation.[4,5] This suggests that general crystallization methods such as changing pH, precipitant, or protein concentration alone cannot always lead to diffraction-quality crystals and that additional factors such as additive type and concentration must also be considered. This can be difficult to address using empirical solution screens, from which knowledge of the underlying interactions between proteins and additives leading to crystallization versus precipitation is difficult to obtain.[6,7]

One approach that has been successful in identifying conditions conducive to crystallization is to characterize protein interactions in terms of the osmotic second virial coefficient (B_{22}), which is defined as[8]

$$\frac{\Pi}{cRT} = \frac{1}{\mathrm{MW}} + B_{22}c + \ldots \quad (1)$$

Π is the osmotic pressure, c is the protein concentration, MW is the protein molecular weight, R is the gas constant, and T is the absolute temperature. As such, B_{22} is a first-order correction to ideal solution behavior that, in this case, accounts for the magnitude and direction of interactions between two protein molecules in solution. Positive B_{22} values indicate an increase in the osmotic pressure of the solution, associated with repulsive interactions, whereas negative B_{22} values indicate the opposite. In a pioneering study a decade ago, George and Wilson observed that solution conditions leading to crystallization for nine soluble proteins gave B_{22} values within the range of −0.8 to −8.0 mol mL g^{-2}, which correspond to weakly attractive protein−protein interactions.[9] On the basis of these results, they proposed this range of B_{22} values as the "crystallization slot", thereby providing a quantitative correlation from which to identify potential crystallization conditions. This has led to further studies of crystallization patterns and interactions for a variety of model proteins aimed at understanding their relationship to B_{22}.[10−16]

Unfortunately, this approach has not been widely adopted for crystallization of novel proteins, in large

* To whom correspondence should be addressed: Department of Chemical Engineering, University of Delaware, Newark, DE 19716. Phone: (302) 831-8989. Fax: (302) 831-4466. E-mail: lenhoff@che.udel.edu.
† Center for Molecular and Engineering Thermodynamics, Department of Chemical Engineering.
‡ Department of Chemistry and Biochemistry.
§ Department of Biological Sciences.

10.1021/cg050013u CCC: $30.25
Published on Web 06/07/2005

part due to experimental limitations. In particular, traditional methods for measuring B_{22}, such as static light scattering, membrane osmometry, and analytical ultracentrifugation, all require significant amounts of protein (typically milligrams of protein per measurement), instrumentation, and effort.[17−19] These requirements are often beyond the limits of what can reasonably be expressed and purified for a given protein. Self-interaction chromatography (SIC), however, allows one to overcome these difficulties in the course of determining B_{22}.[20] By immobilizing the protein of interest onto chromatographic particles, packing these into a column, and injecting a pulse of the same protein into the running buffer, one can gauge the relative degree of interaction between proteins as a function of solution conditions in terms of their retention, which can be related to B_{22}.[21] Importantly, SIC reduces the amount of protein necessary to make such measurements by at least an order of magnitude relative to conventional methods, thereby making it tractable for studying new proteins. With use of an HPLC and autosampler, this process can be automated and the amount of sample per measurement can be significantly reduced.

Regardless of the method used to measure B_{22}, the use of interaction measurements to guide crystallization experiments has been limited thus far mainly to model proteins. Here we show that such a rational approach to optimizing crystallization conditions can also be effective for novel proteins, ultimately providing new insights into structure−function relations. The protein studied is calcium- and integrin-binding protein (CIB), a Ca^{2+} binding protein with significant homology to other Ca^{2+} regulatory proteins such as calmodulin and calcineurin B.[22,23] It is expressed in human platelets and interacts specifically with the integrin α_{IIb} subunit cytoplasmic domain, where it is thought to play a role in signaling pathways related to platelet activation and spreading.[24,25] In crystallization efforts by conventional methods, initial screens led to crystal formation in only a few cases, but overall crystal growth and quality were limited by significant precipitation. We show how the use of additives such as alkanediols, guided by SIC measurements of protein osmotic second virial coefficients, can inhibit precipitation and improve solubility. These results, in combination with isothermal titration calorimetry (ITC) and solubility measurements, provide insight into the specificity of protein−additive interactions during crystallization. Our results also exemplify the use of SIC as part of a rational approach for crystallization of novel proteins. By expanding the range of solution conditions used to include precipitants and additives not originally considered in conventional screens, we were able to examine the effects of each systematically to find improved crystallization conditions for CIB using ultracentrifugal crystallization (UC).[26]

Materials and Methods

Materials. 1-Ethyl-3-(3-dimethylaminopropyl)carbodiimide (EDC; 22980), *N*-hydroxysuccinimide (NHS; 24500), Tris-(2-carboxyethyl)-phosphine hydrochloride (TCEP; 20460) and the Micro BCA Protein Assay kit (23231, 23232, 23234) were obtained from Pierce. 2-(*N*-Morpholino)ethanesulfonic acid (MES; M8250), sodium malonate (M4795), sodium formate (F4166), sodium acetate (241245), calcium chloride (223506), and 1-propanol (402893) were from Sigma. Butane-1,4-diol (AC10763), butane-1,2-diol (AC17599), pentane-1,2-diol (AC12329), pentane-1,5-diol (AC12995), hexane-1,2-diol (AC20013), hexane-1,6-diol (AC16035), heptane-1,7-diol (AC12035), and octane-1,2-diol (AC20014) were from Fisher Scientific. AF-Amino-650M particles (08002) were from Tosoh Biosep. 3 × 50 mm borosilicate glass microcolumns (993301) were from P. J. Cobert and Associates.

Expression and Purification. Cloning, expression, and purification of CIB have been described previously.[27,28] Aliquots of purified CIB at concentrations ranging from 10 to 30 mg/mL were flash frozen using liquid N_2 in 30% sucrose and stored at −80 °C until use. Unless otherwise stated, measurements were made using 20 mM MES, pH 6 buffer containing 0.1 mM TCEP and 1 mM $CaCl_2$ to stabilize CIB. TCEP was added immediately before use from a 100 mM stock solution stored at −80 °C; all buffer solutions containing TCEP were used within 24 h. Protein concentrations were measured using a Perkin-Elmer Lambda 2 UV−visible spectrophotometer.

Self-Interaction Chromatography. Particles carrying immobilized CIB for SIC were prepared using EDC and NHS to attach CIB covalently via its surface-accessible carboxylic acid groups to the primary amine groups on the Tosoh Biosep AF-Amino-650M particle surface.[29] A total of 0.5 mL of settled particles were washed extensively with water and resuspended in 8 mL of 20 mM MES, pH 6 buffer containing 2 mg of NHS and 60 mg of EDC. A total of 2 mL of a 15 mg/mL CIB solution was then added, and the suspension was allowed to mix by gentle agitation on a rotary mixer at room temperature for 8 h. The particles were collected by passing the suspension over a glass frit with a 0.2 μm Supor-200 membrane filter (Pall). The particles were washed 3 times with 50 mL aliquots of 20 mM MES, pH 6 buffer. Samples were collected from each wash, and the particles were stored at 4 °C. Immobilized protein concentrations were determined by a mass balance based on the residual protein in the wash solutions using values determined from a Bradford assay as well as from a direct measurement of the protein immobilized on the particles using the micro BCA method as per the manufacturer's instructions. A modified Bradford assay was preferable to conventional absorbance values at 280 nm due to the low concentrations of CIB typically present in the wash steps and the small number of aromatic residues in CIB. Column packing, calibration, and sample runs were essentially as described previously, using a 0.35 mL borosilicate glass microcolumn.[21] Injection concentrations of 5 mg/mL CIB and volumes of 50−100 μL were found to give reproducible results.

To correct for differences in diffusivity occurring with high concentrations of alkanediols, the effective flow rate was reduced in inverse proportion to the viscosity of the mixture:

$$F_2 = F_1\left(\frac{\mu_1}{\mu_2}\right) \tag{2}$$

F_2 is the actual flow rate, F_1 is the initial flow rate, μ_1 is the initial viscosity, and μ_2 is the viscosity of the alkanediol−water mixture. A similar approach was used in measuring osmotic second virial coefficients by SIC for ribonuclease A at high poly(ethylene glycol) (PEG) concentrations.[13] Viscosity data for alkanediol−water mixtures are available in the literature.[30−38] All measurements were made at 22 ± 2 °C using an ÄKTA Explorer HPLC unit with A-900 autosampler (Amersham Biosciences). Data were collected and processed using the Unicorn 4.00.16 software package. Each retention volume used in determining B_{22} was an average of three independent measurements to ensure reproducibility with an error of less than 5%.

Chromatographic retention is typically characterized in terms of the retention factor k'[39]:

$$k' = \frac{V_r - V_o}{V_o} \tag{3}$$

Here V_r refers to the retention volume of the solute as it passes through the column at a given solution condition of interest, and V_o refers to the retention volume at a solution condition at which the solute does not interact with the particle surface. Estimates of V_o were made using 1% (v/v) acetone and corrected for differences in effective pore volume due to immobilized protein as described previously.[21] B_{22} was calculated according to the relation[13,21]

$$B_{22} = B_{22}^{HS} - \frac{k'}{\rho_s \phi} \quad (4)$$

B_{22}^{HS} is the excluded volume contribution, ρ_s is the immobilization density or the amount of protein immobilized per unit accessible surface area of the particle,[21] and the phase ratio ϕ is the total accessible surface area of the pore space per unit volume of mobile phase, which is a property of the chromatographic material used.[40] Therefore, the product $\rho_s\phi$ is a measure of the concentration of immobilized protein available to interact with mobile protein molecules. A detailed discussion of the methods used for preparing a column and determining the necessary parameters used in eq 4 to calculate B_{22} values from SIC data has been provided previously,[21] the key observation being that these parameters can be determined independently, allowing B_{22} to be determined without the use of any adjustable parameters. B_{22}^{HS} was determined from correlations for globular, soluble proteins based on their molecular weights assuming CIB to be spherical with a monomer molecular mass of 21586 Da.[41] The amount of CIB immobilized was 14−18 mg/mL settled particles, corresponding to an approximate surface coverage of 19%. For the Tosoh Biosep AM-Amino 650M particles, ϕ was estimated as 16.4 m^2/mL mobile phase.[40]

Ultracentrifugal Crystallization. Ultracentrifugal crystallization was carried out using a Beckman Optima MAX benchtop ultracentrifuge with a TLS-55 rotor. For crystallization, 50 μL of a 10 or 20 mg/mL CIB solution was added to a mixture of concentrated additive solution and buffer. To this, concentrated precipitant solution was added such that the total volume was 200 μL, thereby adjusting the concentrations of all components to their desired values, and the solution was mixed briefly. On the basis of previous work with other soluble proteins, the centrifugation speed was chosen so that the protein would sediment completely within 48 h; a speed of 45 000 rpm was chosen, based on a sedimentation coefficient of 2.23×10^{-13} s for CIB,[13,26] which was calculated under the assumption of a compact, spherical protein.[42] Protein partial specific volumes and solution densities for CIB in a concentration range of 5−20 mg/mL were determined using an Anton Paar DMA 60 density meter using methods described previously.[43] After centrifugation, samples were examined by optical microscopy using an Olympus BHT microscope with camera and then stored at 4 °C to determine what further changes in phase behavior might occur with time. Crystals were identified based on their appearance as well as by their ability to refract polarized light.

Solubility Measurements. To measure solubility limits, concentrated CIB, additive, precipitant, and buffer solutions were mixed gently with a pipet such that the total volume was 4 μL. Drops were then placed on glass coverslips and sealed using conventional hanging-drop techniques against a 500 μL reservoir at the same additive and precipitant concentrations. Solutions were allowed to stand at 20 °C until visible crystallization or precipitation was observed. On the basis of the observed phase behavior, approximate precipitation boundaries were identified and 100 μL samples at corresponding solution conditions were prepared. These were subjected to ultracentrifugation as described above. The concentration of CIB remaining in the supernatant after centrifugation was determined by a modified Bradford assay. All solutions were also examined by optical microscopy to determine whether precipitates or crystals had formed.

Isothermal Titration Calorimetry. Critical micelle concentration (CMC) values for alkane-1,2-diols were measured by ITC using a Microcal isothermal titration calorimeter. In a typical experiment, 20 μL samples of alkane-1,2-diol were injected into a 1.5 mL sample chamber containing sample buffer at a fixed CIB concentration. The injections were chosen such that the final concentration of alkane-1,2-diol spanned a range of 0.02−2 M to include concentrations above and below the CMC; for *n*-octyl-β-D-glucoside, the relevant concentration range was 0.2−200 mM. By comparing the change in heat released with change in surfactant concentration, the CMC can be determined from the maximum in the heat profile. Heats of dilution using buffer injections were negligible.

For determining the precipitation threshold of CIB, the reservoir concentration was fixed at 3 M sodium formate, 15% (v/v) alkanediol, and injections were made using a concentrated CIB solution in sample buffer. The maximum in the heat profile was attributed to protein aggregation, as the resultant CIB concentration was in good agreement with the observed precipitation threshold determined as described above for propane-1,3-diol. Heats of dilution using buffer alone were negligible.

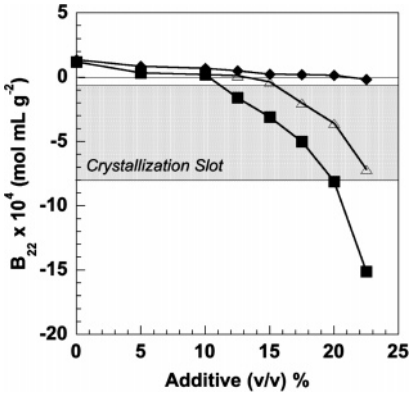

Figure 1. Values of the osmotic second virial coefficient for CIB as a function of additive type and concentration: (■) 1-propanol, (△) 2-methyl-propane-1,2-diol, and (◆) propane-1,2-diol. Unless otherwise stated, all measurements were made using 20 mM MES, pH 6 buffer containing 0.1 mM TCEP and 1 mM $CaCl_2$.

Results

Interactions using 1-Propanol and Alkanediols. Initially, CIB crystals were obtained by conventional hanging drop crystallization using Hampton Crystal Screens 1 and 2 in solutions containing more than 10% (v/v) of 1-propanol in combination with sodium chloride or PEG 4000.[27] These crystals were fragile and of low diffraction quality. Varying solution conditions using these components often led to significant precipitation, thereby complicating initial crystal improvement. We hypothesized that this might be due to 1-propanol because organic solvents such as ethanol and propanol are known protein denaturants that are thought to cause partial unfolding by interacting specifically with hydrophobic side chains of proteins at high concentrations, thereby disrupting local water structure.[44,45] We therefore focused our attention on a class of structurally similar compounds, alkanediols, which have been successful in promoting the crystallization of soluble and membrane proteins.[4] Addition of hydroxyl groups enhances the compatibility between the alkanediols and water, which in turn reduces their preferential interaction with hydrophobic side chains of proteins.[46−48] Figure 1 shows a comparison of the protein interactions in the presence of polyhydric variants of 1-propanol. In all cases, B_{22} values measured by SIC for CIB are an

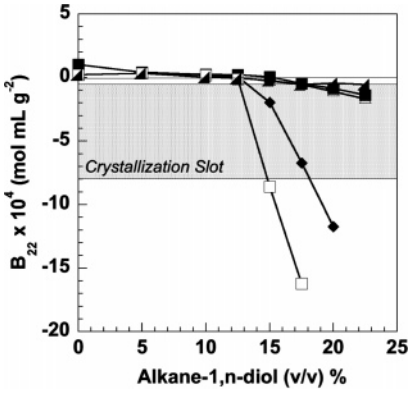

Figure 2. Effect of alkane-1,*n*-diol chain length and concentration on CIB interactions. (▲) DMSO, (■) butane-1,4-diol, (△) pentane-1,5-diol, (◆) hexane-1,6-diol, (□) heptane-1,7-diol.

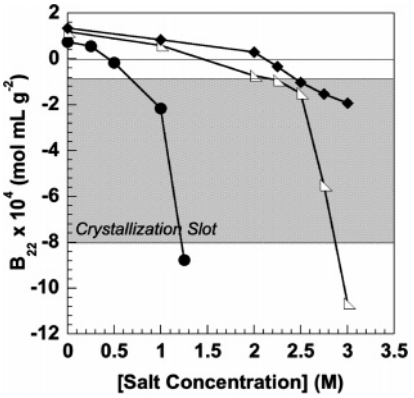

Figure 3. Effect of salt type and concentration on CIB interactions. (●) Sodium malonate, (△) sodium formate, (◆) sodium acetate.

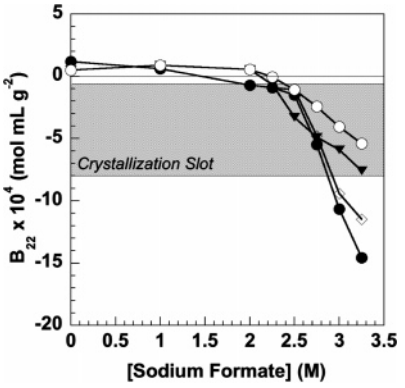

Figure 4. Effect of butane-1,4-diol on CIB interactions with increasing sodium formate concentration. (●) 0% (v/v) butane-1,4-diol, (◇) 5% (v/v) butane-1,4-diol, (▼) 10% (v/v) butane-1,4-diol, (○) 15% (v/v) butane-1,4-diol.

average of three independent measurements, with variability of less than 5% in retention time. The interactions in 1-propanol show little effect of the additive at concentrations less than about 10%, but higher concentrations give rise to a relatively steep increase in attraction (more negative B_{22} values) that pushes the virial coefficient beyond the crystallization slot by nearly 20%. Adding a hydroxyl group (propane-1,2-diol) largely eliminates the tendency toward attractive CIB interactions at high volume fractions, whereas adding a methylene and a hydroxyl group (methylpropanediol) causes an intermediate decrease in attractive interactions, with several points falling within the crystallization slot. This weaker attraction would be expected to be conducive to crystallization, although crystallization attempts with methylpropanediol led to a mixture of microcrystals and precipitate.

On the basis of these results, a homologous series of alkane-1,*n*-diols was examined in an effort to modulate the interactions further. Neither extending the chain length from three to five methlyene units nor using DMSO leads to a significant change in CIB interactions (Figure 2). However, the longer chain hexane-1,6-diol and heptane-1,7-diol cause a sharp increase in attractive interactions above 15% (v/v), with a much narrower range of solution conditions leading to values within crystallization slot. Crystallization attempts with hexane-1,6-diol or heptane-1,7-diol led to liquid−liquid-phase separation and precipitation, whereas use of DMSO or other short-chain alkane-1,*n*-diols such as butane-1,4-diol in crystallization was successful in combination with salts as discussed below.

Influence of Salts on Interactions. Salts of organic acids, such as sodium formate or sodium malonate, have been shown to be useful in protein crystallization, being as effective as more commonly used precipitants such as ammonium sulfate in crystallization screens for soluble proteins.[49] This effectiveness results from their behaving as kosmotropes in the Hofmeister series, which increases the surface tension of water and protein stability,[50−52] but these anions also have the advantage of not forming complexes with Ca^{2+}, which is necessary for stabilizing CIB at concentrations relevant for crystallization. Sodium malonate, formate, and acetate are all effective at inducing attractive interactions for CIB (Figure 3), with malonate and formate ultimately giving rise to very steep profiles within and beyond the crystallization slot. However, both formate and acetate display relatively gradual variations within the upper portion of the slot, and consequently formate yields a fairly wide range of solution conditions within the crystallization slot. Ultracentrifugal crystallization attempts on CIB using 2.7−3 M sodium formate led to significant crystal formation, although this generally occurred as showers of small crystals rather than distinct, larger ones.

Combined Effect of Salts and Alkanediols. We sought to improve crystallization of CIB by adding alkanediols to attenuate the protein attraction at high salt concentrations. Similar approaches have been used in improving crystallization of other soluble proteins.[53−55] For butane-1,4-diol in combination with sodium formate (Figure 4), increasing the butane-1,4-diol concentration reduces attractive CIB interactions at high salt concentrations, consistent with its primary effect as a stabilizer as shown in Figure 2. DMSO was also effective in promoting crystal formation in combination with sodium formate, leading to crystals of improved diffraction quality.[27] On the basis of the SIC results in Figure 2, one would expect it to behave similarly to the alkane-1,*n*-diols, notably butane-1,4-diol, as a stabilizer at high volume fractions as well.

Overall, the stabilizing effects of the alkane-1,*n*-diols at high salt concentrations exhibit a complex dependence on alkyl chain length. This can be seen more clearly in terms of the precipitation threshold, defined

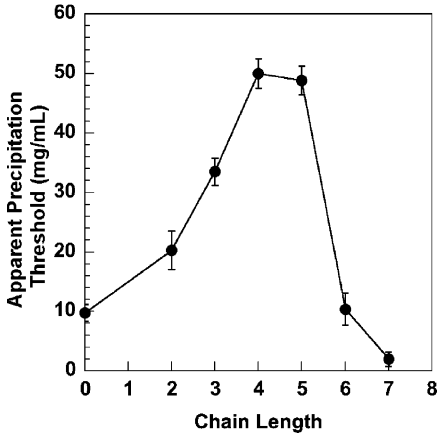

Figure 5. Effect of alkane-1,*n*-diol chain length on observed precipitation threshold in the presence of 3 M sodium formate. Each point represents the average of three independent measurements of CIB concentration in the supernatant. In each case, alkanediol concentrations were fixed at 15% (v/v). Alkyl chain length refers to the number of carbon atoms in the chain, including those with hydroxyl groups.

here as the appearance of a macroscopic, irreversible precipitate immediately following an increase in the salt concentration. This is distinct from crystallization conditions, in which a transparent solution was observed over the course of one week, during which time crystal formation occurred. The effects of the various alkane-1,*n*-diols on the CIB precipitation threshold at 3 M sodium formate are summarized in Figure 5 and indicate a maximum at $n = 4-5$ and a subsequent sharp decrease in the precipitation threshold for $n = 6$ and 7. Similar experiments with DMSO also led to improved CIB solubility, falling between those of propane-1,3-diol and butane-1,4-diol (results not shown). A concentration of 3 M sodium formate was chosen since it represents a value typical for the range of concentrations that were most effective in promoting crystal formation as discussed below. Thus, short-chain alkanediols improved CIB solubility by inhibiting precipitation up to a chain length of 4−5, whereas longer chains such as hexane-1,6-diol and heptane-1,7-diol actually reduced CIB solubility and enhanced precipitation relative to 3 M sodium formate alone.

Alkane-1,2-diols also attenuated attractive CIB interactions in formate solutions (Figure 6). Interestingly, the longer-chained hexane- and octane-1,2-diol were necessary to obtain interactions within the crystallization slot at high formate concentrations, whereas for the alkane-1,*n*-diols, the smaller butane-1,4-diol was preferred. The specificity for a particular chain length in the case of the alkane-1,2-diols in balancing attractive CIB interactions at high formate concentrations with reduced precipitation relative to the alkane-1,*n*-diols may be a result of differences in surface activity; longer-chain alkane-1,2-diols such as hexane-1,2-diol have clearly defined CMCs, whereas the alkane-1,*n*-diols and shorter-chain alkane-1,2-diols generally do not.[56,57] Therefore, it may be that long-chain alkane-1,2-diols such as hexane-1,2-diol associate more strongly with hydrophobic regions of CIB and thereby enhance crystallization versus precipitation. Crystallization attempts with hexane-1,2-diol also led to significant crystal formation.

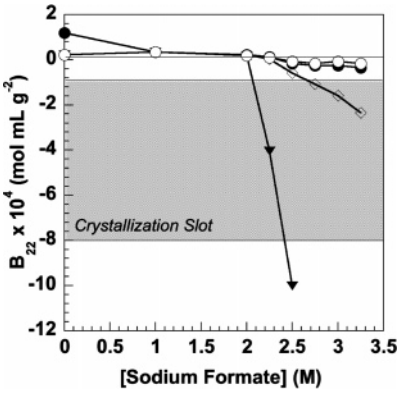

Figure 6. Effect of alkane-1,2-diol at 5% (v/v) on CIB interactions with increasing sodium formate concentration. (○) Butane-1,2-diol, (●) pentane-1,2-diol, (◇) hexane-1,2-diol, (▼) octane-1,2-diol.

Table 1. Summary of Ultracentrifugal Crystallization Conditions for CIB Based on SIC Experiments*

salt conc [M]	$B_{22} \times 10^4$ [mol mL g^{-2}]	phase separation
Sodium Malonate		
0.25	0.56	none
0.5	−0.17	none
1	−2.2	microcrystals[a]
1.25	−8.8	crystals + precipitate
Sodium Malonate + 10% (v/v) Butane-1,4-diol		
0.5	0.84	none
1	−0.8	none
1.25	−4.6	microcrystals[b]
1.5	−7.1	crystals + precipitate
Sodium Formate		
2.25	−0.93	none
2.5	−1.5	microcrystals
2.75	−5.5	crystals
3	−10.7	precipitate
Sodium Formate + 10% (v/v) Butane-1,4-diol		
2.25	−0.67	none
2.5	−3.3	crystals
2.75	−4.9	crystals[d]
3	−5.9	crystals
Sodium Formate + 5% (v/v) Hexane-1,2-diol		
2.5	−4.1	none
2.75	−9.6	none
3	−19.0	microcrystals
3.25	−19.0	microcrystals[c]

* All crystallization solutions contained 10 mg/mL CIB in 20 mM MES, pH 6 buffer with 0.1 mM TCEP and 1 mM $CaCl_2$. The superscripts a−d refer to the panels in Figure 7, where images for representative cases of CIB phase separation and crystal formation are shown.

Ultracentrifugal Crystallization. On the basis of our SIC results, 20 solution conditions encompassing the range of precipitants and additives used were chosen for which CIB virial coefficients fell within or near the crystallization slot and subjected to ultracentrifugal crystallization; the solution conditions used, their corresponding B_{22} values, and observed CIB phase behavior for each case are summarized in Table 1. In general, the SIC results indicated that adding shorter-chain alkane-1,*n*-diols such as butane-1,4-diol mitigates the strong protein attraction at high salt concentrations, leading to a wider range of solution conditions conducive to crystallization (Figure 4); longer-chain homologues are more effective in the case of the alkane-1,2-diols, notably hexane-1,2-diol (Figure 6). However, it is also clear from these results that the choice of salt, in this

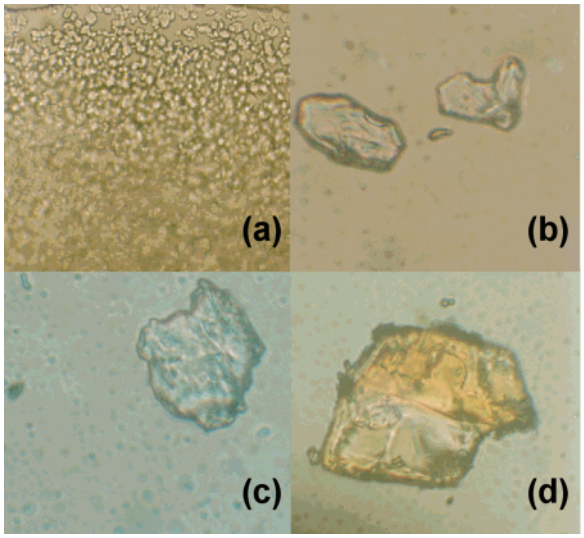

Figure 7. Crystallization patterns for CIB using various organic salts and alkanediols. All crystallization solutions contained 10 mg/mL CIB in 20 mM MES, pH 6 buffer with 0.1 mM TCEP and 1 mM $CaCl_2$. Corresponding osmotic second virial coefficients for each panel are shown in Table 1. Images were taken using an Olympus BHT microscope. The approximate size of each panel is 200 × 200 μm. (a) 1 M sodium malonate. (b) 1.25 M sodium malonate with 10% (v/v) butane-1,4-diol. (c) 3.25 M sodium formate with 5% (v/v) hexane-1,2-diol. (d) 2.75 M sodium formate with 10% (v/v) butane-1,4-diol.

case sodium malonate or sodium formate, was crucial to promoting sufficiently attractive B_{22} values within the crystallization slot (Figure 3).

Examples of crystals obtained by UC for different sets of conditions are shown in Figure 7. The improvement in crystal growth and reduction of precipitation in the presence of alkanediols is evident for both malonate and formate, which resulted in crystals that were approximately 40 μm in size for 1.25 M sodium malonate with 10% (v/v) butane-1,4-diol (Figure 7b) and approximately 50−100 μm in size for 3.25 M sodium formate with 5% (v/v) hexane-1,2-diol (Figure 7c) and 2.75 M sodium formate with 10% (v/v) butane-1,4-diol (Figure 7d) as compared to the microcrystals obtained for 1 M sodium malonate alone (Figure 7a). Similar patterns of microcrystal formation were observed for 2.5−3 M sodium formate solutions as well (results not shown). A major advantage of UC is that for a typical run, crystals form within 48 h, allowing one to screen potential solution conditions for crystallization rapidly in conjunction with SIC while matching solution conditions between the two methods. Potentially successful crystallization conditions can then be improved upon by other methods such as vapor diffusion or microdialysis, although in these cases the solution conditions may change from those giving rise to crystallization slot B_{22} values.

Discussion

Our SIC results for CIB led to a wide range of conditions that, as judged by the crystallization slot criterion, appeared suitable for crystallization. These included use of organic salts, such as sodium formate and sodium malonate, as well as polyhydric alcohols, such as hexane-1,2-diol or butane-1,4-diol, many of which are not included in typical protein crystallization screens such as the Hampton Crystal Screen 1 and 2. By interpreting the observed phase behavior in terms of B_{22}, we gain much useful information about the interactions between CIB molecules as a function of solution conditions. This allows for a refinement of crystallization conditions in a systematic manner, where the effects of individual solution components on the measured B_{22} can be examined. For CIB, this is a particularly useful approach, since initial crystallization screens were largely unsuccessful. As an example, Crystal Screen 1 contains two potential crystallization conditions using sodium formate: 4 M sodium formate, unbuffered (condition 33) and 2 M sodium formate, 0.1 M sodium acetate, pH 4.6 (condition 34). Differences in pH notwithstanding, the CIB interactions at pH 6 (Figure 3) first become attractive near 2 M sodium formate and are strongly attractive by 3 M sodium formate, where the virial coefficients are well beyond the crystallization slot. Thus, the window of solution conditions from 2 to 3 M sodium formate, which may be most conducive to crystal formation, is missed by conventional screens. Likewise, the only alkanediol apart from MPD available in Crystal Screens 1 and 2, hexane-1,6-diol, led to strongly attractive CIB interactions and subsequent precipitation (Figure 2), whereas the SIC analysis indicated the specificity of alkanediol structure as being important to provide stability for CIB at the high sodium formate concentrations necessary for crystal formation, namely, butane-1,4-diol and hexane-1,2-diol. DMSO, which is not included in the Hampton screens either, is also able to improve CIB crystal formation in a fashion similar to either butane-1,4-diol or hexane-1,2-diol (Figure 2). Therefore, it may be advantageous to expand initial crystallization screens to include a wider range of organic salts and alkanediols or DMSO, particularly with proteins such as CIB that display poor solubility and crystal growth. Overall, the good agreement between crystallization results and osmotic second virial coefficients measured by SIC (Table 1) provides further justification of the crystallization slot concept for soluble proteins.

The effect that alkanediols have on protein structure and interactions is still an area of active research. 2-Methyl-2,4-pentanediol (MPD) is perhaps the best known alkanediol used for protein crystallization, and its effects on the crystallization of soluble proteins have been studied extensively. Pittz and Timasheff found that MPD affected the crystallization of bovine pancreatic ribonuclease A mainly through preferential hydration of the protein, suggesting that specific MPD interactions with hydrophobic regions of the protein were not the dominant effect leading to crystallization.[58] Rather, at high volume fractions of MPD, RNase A undergoes phase separation, which in this case is crystallization, at pH 5.8 to avoid contact with MPD. However, a broad survey of proteins for which detailed structural information is available, including atomic coordinates for MPD, found that MPD demonstrated a preference for solvent-exposed hydrophobic residues.[59] Direct MPD interaction with these residues would reduce unfavorable solvent-exposed hydrophobic surface area, thereby

facilitating preferential protein hydration and eventual crystallization of the stabilized structure.

Interestingly, bovine brain calmodulin, which shares significant homology to CIB, was crystallized using MPD as well.[60] Given that calmodulin and CIB both have an extensive hydrophobic cleft, it seems likely that the alkanediols used act mainly as protein stabilizers rather than as precipitants at high salt concentrations. This is supported by the relatively small number of attractive B_{22} values observed in Figure 2 for the majority of alkane-1,*n*-diols used up to 25% (v/v), whereas Figure 4 shows that adding butane-1,4-diol at high sodium formate concentrations diminishes attractive CIB interactions, leading to a wider range of values within the crystallization slot. Furthermore, the apparent precipitation limit for CIB is dependent on the chain length of the alkanediol, as shown in Figure 5. This result is in agreement with additional measurements by ITC for propane-1,3-diol, in which the maximum in the heat profile with increasing CIB injections coincides with the appearance of precipitate and is shifted to higher CIB concentrations relative to 3 M sodium formate solution alone (results not shown). Overall, these results indicate the specificity of alkanediol structure in stabilizing CIB during crystallization and suggest that complementarities of shape may be a factor in determining which alkanediols are most effective.

It is also noteworthy that the trend of improved crystal growth follows that of increasing precipitation threshold, suggesting that eliminating deleterious strong attraction, potentially due to the hydrophobicity of CIB, is beneficial in allowing crystal growth to proceed. In this sense, the alkanediol may act similarly to surfactants in crystallization of membrane proteins, where solubilization reduces precipitation or aggregation and allows the controlled association of protein molecules into a protein crystal. Numerous experimental and theoretical investigations into the mixing of polyhydric and monohydric alcohols with water suggest that longer chains allow formation of micelle-like aggregates in solution, and the degree of association is reduced by adding hydroxyl groups.[31,61−63] Therefore, the effect of alkane-1,*n*-diols on CIB crystallization may reflect a balance between modulating water structure through the hydroxyl groups and association with hydrophobic regions on the protein surface, which would depend on chain length.

An interesting analogous approach to crystallization is through use of alkane-1,2-diols, which, as mentioned before, display surface activity with a CMC of 0.81 M in the case of hexane-1,2-diol.[57] Unlike the alkane-1,*n*-diols, longer chain alkane-1,2-diols may act as surfactants and thus show a stronger association with the hydrophobic regions of a particular protein such as CIB. However, this association with CIB competes with self-association to form micelles at the CMC. This competition is expected to be especially significant at the high salt concentrations typically used in crystallization, which substantially reduce the CMC of most nonionic surfactants.[64] Therefore, should there be specific interaction between hexane-1,2-diol and CIB, one would expect an increase in CMC for hexane-1,2-diol in the presence of CIB. Using ITC, the change in CMC for hexane-1,2-diol with increasing concentrations of CIB was determined (Figure 8). With increasing CIB concentration, the maximum in the heat profile shifts to higher hexane-1,2-diol concentrations; this demonstrates specific interactions between the two components, suggesting that approximately 27 molecules bind per CIB molecule, although the exact number of bound hexane-1,2-diol molecules should be viewed with some caution due in part to the changes measured being small relative to the CMC. This is likely a consequence of hexane-1,2-diol being weakly amphiphilic, thus having a CMC that is orders of magnitude larger than those of other typical nonionic surfactants. Additional experiments using *n*-octyl-*β*-D-glucoside show a more pronounced increase in CMC, although with a smaller number of bound surfactant molecules (results not shown).

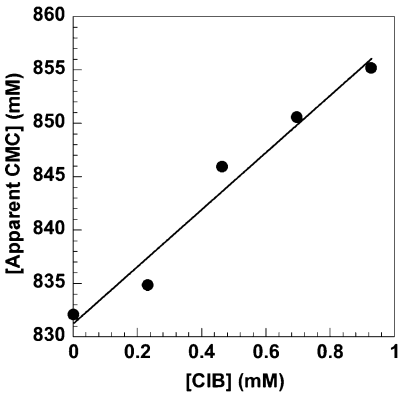

Figure 8. Increase in apparent CMC for hexane-1,2-diol in the presence of CIB as determined by ITC. The equation of the best-fit line to the data is [apparent CMC] = 26.7 [CIB] + 831, suggesting that approximately 27 hexane-1,2-diol molecules are associated with each CIB molecule.

The amount of bound hexane-1,2-diol is higher than reported for other nonionic surfactants binding to soluble proteins.[65,66] However, the higher number is consistent with previous observations for MPD and other small organic molecules, where the smaller size and increased flexibility allow more efficient packing around hydrophobic regions of the protein surface.[59,67−69] The recent structure of CIB also reveals a solvent-exposed hydrophobic cleft, similar to that of calmodulin, which could also allow direct interaction with several surfactant molecules.[28] The larger size of other nonionic surfactants such as *n*-octyl-*β*-D-glucoside or Triton X-100 may lead to lower accessibility and thus less room to accommodate bound surfactant molecules. Therefore, it is likely that longer-chain alkane-1,2-diols behave as intermediate cases between weakly associating compounds such as MPD and alkane-1,*n*-diols and nonionic surfactants such as *n*-octyl-*β*-D-glucoside. This would also explain why much lower concentrations are necessary to have an effect on CIB interactions and strengthen the argument that specific interactions are important for reducing precipitation and enhancing crystal formation.

Conclusions

Our results demonstrate for CIB that additives play a key role in modulating the protein−protein interactions necessary to improve crystallization at high salt concentrations. The value of this work lies in the

systematic investigation of additive and precipitant effects on CIB virial coefficients, facilitated by use of self-interaction chromatography, to distinguish the role that each component plays in CIB crystallization. In particular, we have shown that alkanediols and DMSO reduce precipitation at high salt concentrations by improving solubility, and from this follows the observed improvement in crystal growth, ultimately leading to diffraction-quality crystals. The differences in alkanediol specificity for CIB are likely due to their surface activity in the case of longer-chain alkane-1,2-diols and complementarity of size in the case of alkane-1,*n*-diols. Therefore, for proteins that display poor solubility or that crystallize in the presence of organic solvents such as 1-propanol, it may be advantageous to expand screening to include use of polyhydric alcohols or DMSO in combination with organic salts such as sodium malonate or formate to improve crystal growth and quality. Overall, understanding how additives control protein−protein interactions, as well as the availability of methods such as self-interaction chromatography to characterize them efficiently, provides a promising approach to the rational crystallization of novel or otherwise difficult proteins.

Acknowledgments. This publication was made possible by NIH Grant P20 RR-15588 from the COBRE program of the National Center for Research Resources, by NASA Grant NAG8-1830, and by NSF Grant BES-0078844. B.W.B. and C.J.B. gratefully acknowledge support through a NIH Chemistry-Biology Interface Training Grant T32 GM-08550; B.W.B. also acknowledges support through an NSF IGERT graduate fellowship DGE−0221651. We thank André Dumetz for useful discussions and assistance.

References

(1) Loll, P. J. *J. Struct. Biol.* **2003**, *142*, 144−153.
(2) Chayen, N. E.; Saridakis, E. *Acta Crystallogr. D* **2002**, *58*, 921−927.
(3) Edwards, A. M.; Arrowsmith, C. H.; Christendat, D.; Dharamsi, A.; Friesen, J. D.; Greenblatt, J. F.; Vedadi, M. *Nat. Struct. Biol.* **2000**, *7*, 970−972.
(4) McPherson, A., *Crystallization of Biological Macromolecules*, 1st ed.; Cold Spring Harbor Press: Cold Springs Harbor, NY, 1999; p 586.
(5) Sousa, R. *Acta Crystallogr. D* **1995**, *51*, 271−277.
(6) Carter, C. W.; Carter, C. W. *J. Biol. Chem.* **1979**, *254*, 2219−2223.
(7) Jancarik, J.; Kim, S. H. *J. Appl. Crystallogr.* **1991**, *24*, 409−411.
(8) McQuarrie, D. *Statistical Mechanics*, 2nd ed.; University Science Books: Sausalito, CA, 2000; p 641.
(9) George, A.; Wilson, W. W. *Acta Crystallogr. D* **1994**, *50*, 361−365.
(10) George, A.; Chiang, Y.; Guo, B.; Arabshahi, A.; Cai, Z.; Wilson, W. W. *Methods Enzymol.* **1997**, *276*, 100−110.
(11) Rosenbaum, D. F.; Zukoski, C. F. *J. Cryst. Growth* **1996**, *169*, 752−758.
(12) Velev, O. D.; Kaler, E. W.; Lenhoff, A. M. *Biophys. J.* **1998**, *75*, 2682−2697.
(13) Tessier, P. M.; Johnson, H. R.; Pazhianur, R.; Berger, B. W.; Prentice, J. L.; Bahnson, B. J.; Sandler, S. I.; Lenhoff, A. M. *Proteins: Struct., Funct., Genet.* **2003**, *50*, 303−311.
(14) Tardieu, A.; Bonnete, F.; Finet, D. S.; Vivares, D. *Acta Crystallogr. D* **2002**, *58*, 1549−1553.
(15) Neal, B. L.; Asthagiri, D.; Velev, O. D.; Lenhoff, A. M.; Kaler, E. W. *J. Cryst. Growth* **1999**, *196*, 377−387.
(16) Hitscherich, C.; Kaplan, J.; Allaman, M.; Wiencek, J.; Loll, P. J. *Protein Sci.* **2000**, *9*, 1559−1566.
(17) Wilson, W. W. *J. Struct. Biol.* **2003**, *142*, 56−65.
(18) Behlke, J.; Ristau, O. *Biophys. Chem.* **2000**, *87*, 1−13.
(19) Schaink, H. M.; Smit, J. A. M. *Phys. Chem. Chem. Phys.* **2000**, *2*, 1537−1541.
(20) Patro, S. Y.; Przybycien, T. M. *Biotechnol. Bioeng.* **1996**, *52*, 193−203.
(21) Tessier, P. M.; Lenhoff, A. M.; Sandler, S. I. *Biophys. J.* **2002**, *82*, 1620−1631.
(22) Hwang, P. M.; Vogel, H. J. *J. Mol. Recognit.* **2000**, *13*, 83−92.
(23) Naik, U. P.; Patel, P. M.; Parise, L. V. *J. Biol. Chem.* **1997**, *272*, 4651−4654.
(24) Naik, M. U.; Naik, U. P. *Blood* **2003**, *102*, 3629−3636.
(25) Naik, U. P.; Naik, M. U. *Blood* **2003**, *102*, 1355−1362.
(26) Lenhoff, A. M.; Pjura, P. E.; Dilmore, J. G.; Godlewski, T. S. *J. Cryst. Growth* **1997**, *180*, 113−126.
(27) Blamey, C.; Naik, U. P.; Bahnson, B. J. *Biophys. J.* **2004**, *86*, 492a.
(28) Blamey, C.; Ceccarelli, C.; Naik, U. P.; Bahnson, B. J. *Protein Sci.* **2005**, *14*, 1214−1221.
(29) Sehgal, D.; Vijay, I. K. *Anal. Biochem.* **1994**, *218*, 87−91.
(30) Yang, C. S.; Ma, P. S.; Zhou, Q. *J. Chem. Eng. Data* **2004**, *49*, 582−587.
(31) Romeo, C. M.; Paez, M. *J. Therm. Anal. Cal.* **2002**, *70*, 263−267.
(32) Lech, T.; Czechowski, G.; Jadzyn, J. *J. Chem. Eng. Data* **2001**, *46*, 725−727.
(33) Jadzyn, J.; Czechowski, G.; Stefaniak, T. *J. Chem. Eng. Data* **2002**, *47*, 978−979.
(34) Czechowski, G.; Rabiega, A.; Jadzyn, J. *Z. Naturforsch., A: Phys. Sci.* **2003**, *58*, 569−572.
(35) Czechowski, G.; Jadzyn, J. *Z. Naturforsch., A: Phys. Sci.* **2003**, *58*, 321−324.
(36) Czechowski, G.; Jadzyn, J. *Z. Naturforsch., A: Phys. Sci.* **2003**, *58*, 317−320.
(37) Jarosiewicz, P.; Czechowski, G.; Jadzyn, J. *Z. Naturforsch., A: Phys. Sci.* **2004**, *59*, 559−562.
(38) Czechowski, G.; Jarosiewicz, P.; Rabiega, A.; Jadzyn, J. *Z. Naturforsch., A: Phys. Sci.* **2004**, *59*, 119−123.
(39) Guiochon, G.; Shirazi, S.; Katti, A., *Fundamentals of Preparative and Nonlinear Chromatography*; Academic Press: New York, 1994; p 701.
(40) DePhillips, P.; Lenhoff, A. M. *J. Chromatogr. A* **2000**, *883*, 39−54.
(41) Neal, B. L.; Lenhoff, A. M. *AIChE J.* **1995**, *41*, 1010−1014.
(42) Lebowitz, J.; Lewis, M. S.; Schuck, P. *Protein Sci.* **2002**, *11*, 2067−2079.
(43) Pjura, P. E.; Paulaitis, M. E.; Lenhoff, A. M. *AIChE J.* **1995**, *41*, 1005−1009.
(44) Gerlsma, S. Y.; Stuur, E. R. *Int. J. Pept. Protein Res.* **1972**, *4*, 377−383.
(45) Timasheff, S. N.; Inoue, H. *Biochemistry* **1968**, *7*, 2501−2521.
(46) Kishore, N.; Sabulal, B. *Faraday Discuss.* **1998**, *94*, 905−911.
(47) Fujita, Y.; Noda, Y. *Bull. Chem. Soc. Jpn.* **1979**, *52*, 2349−2352.
(48) Franks, F.; Ives, D. J. G. *Q. Rev. Chem. Soc.* **1966**, *20*, 1−44.
(49) McPherson, A. *Protein Sci.* **2001**, *10*, 418−422.
(50) Yamniuk, A. P.; Nguyen, L. T.; Hoang, T. T.; Vogel, H. J. *Biochemistry* **2004**, *43*, 2558−2568.
(51) Kaushik, J. K.; Bhat, R. *Protein Sci.* **1999**, *8*, 222−233.
(52) Busby, T. F.; Atha, D. H.; Ingham, K. C. *J. Biol. Chem.* **1981**, *256*, 2140−2147.
(53) Ebel, C.; Faou, P.; Zaccai, G. *J. Cryst. Growth* **1999**, *196*, 395−402.
(54) Tanaka, S.; Ataka, M.; Kubota, T.; Soga, T.; Homma, K.; Lee, W. C.; Tanokura, M. *J. Cryst. Growth* **2002**, *234*, 247−254.
(55) Becker, M.; Stubbs, M. T.; Huber, R. *Protein Sci.* **1998**, *7*, 580−586.
(56) Elsachouri, M.; Hajji, M. S.; Salem, M.; Essassi, E. M. *Faraday Discuss.* **1995**, *91*, 4105−4109.
(57) Hajji, S. M.; Errahmani, M. B.; Coudert, R.; Durand, R. R.; Cao, A.; Taillandier, E. *J. Phys. Chem.* **1989**, *93*, 4819−4824.
(58) Pittz, E. P.; Timasheff, S. N. *Biochemistry* **1978**, *17*, 615−623.
(59) Anand, K.; Pal, D.; Hilgenfeld, R. *Acta Crystallogr. D* **2002**, *58*, 1722−1728.

(60) Babu, Y. S.; Bugg, C. E.; Cook, W. J. *J. Mol. Biol.* **1988**, *204*, 191−204.
(61) Pangali, C.; Rao, M.; Berne, B. J. *J. Chem. Phys.* **1979**, *71*, 2982−2990.
(62) Pangali, C.; Rao, M.; Berne, B. J. *J. Chem. Phys.* **1979**, *71*, 2975−2981.
(63) Grossmann, G. H.; Ebert, K. H. *Ber. Bunsen Phys. Chem.* **1981**, *85*, 1026−1029.
(64) Tanford, C. *The Hydrophobic Effect*, 2nd ed.; John Wiley and Sons: New York, 1982; p 234.
(65) Sukow, W. W.; Sandberg, H. E.; Lewis, E. A.; Eatough, D. J.; Hansen, L. D. *Biochemistry* **1980**, *19*, 912−917.
(66) Kragh-Hansen, U.; Hellec, F.; de Foresta, B.; le Maire, M.; Moller, J. V. *Biophys. J.* **2001**, *80*, 2898−2911.
(67) Mattos, C.; Ringe, D. *Nat. Biotechnol.* **1996**, *14*, 595−599.
(68) Mattos, C.; Ringe, D. *Curr. Opin. Struct. Biol.* **2001**, *11*, 761−764.
(69) Tanford, C. *J. Mol. Biol.* **1972**, *67*, 59−72.

CG050013U